

International Conference on Space Optics—ICSO 2014

La Caleta, Tenerife, Canary Islands

7–10 October 2014

Edited by Zoran Sodnik, Bruno Cugny, and Nikos Karafolas



MTG FCI visible detector detection chain description and preliminary results

S. Demiguel

T. Gilbert

J. L. Canaud

A. Artinian

et al.



icso proceedings



MTG FCI VISIBLE DETECTOR DETECTION CHAIN DESCRIPTION AND PRELIMINARY RESULTS

S. Demiguel¹, T. Gilbert¹, J.L. Canaud¹, A. Artinian¹, M. Wilson².
¹Thales Alenia Space, Cannes, France. ²European Space Agency, Netherland

INTRODUCTION:

The next generation of geostationary meteorological satellites is being developed in the frame of Meteosat Third Generation (MTG) ESA program [1] where Thales Alenia Space is prime. The novel Flexible Combined Imager (FCI) instrument exhibit in particular a detection block including 17 channels from the visible to the far infrared working in snapshot mode at high frame rate (~2.65kHz) with a ground resolution between 0.5 - 2km. The full description of FCI optical design and performance features can be found in paper referenced [2]. A functional diagram is presented in Fig 1. The optical signal is spectrally separated in two at the telescope output to be driven to a warm assembly maintained at ambient temperature for the five visible channels, and to another assembly cooled down at 60K for the three NIR and nine infrared ones. The infrared block composed of 4 detectors assemblies based on HgCdTe material hybridized on CMOS ROIC circuit while the visible block contained a CMOS image sensor working at high pixel frequency (~4MHz). Each detector assemblies exhibits one unique analogue output. The video signals are sent to Video Control Units (VCU) to be buffered and digitalized.

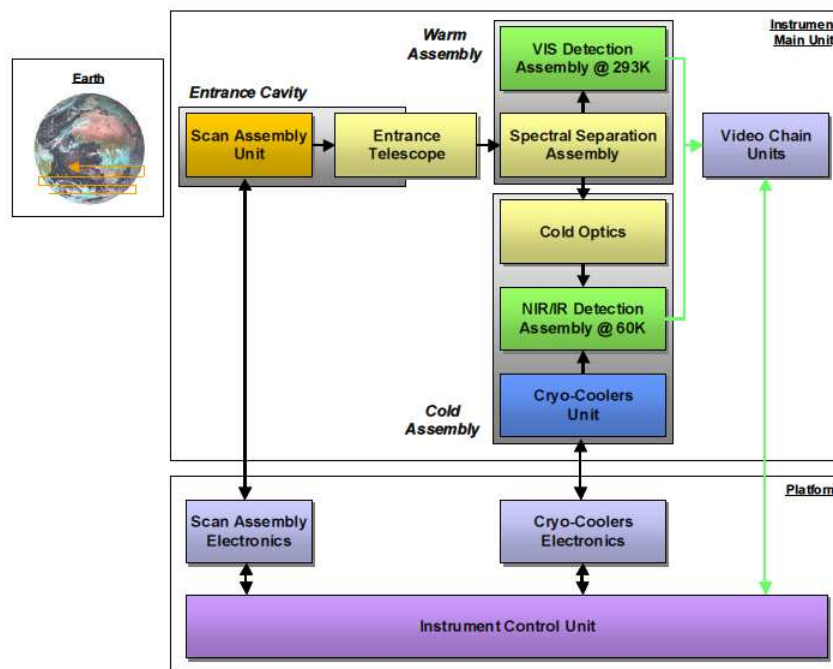


Fig. 1. MTG FCI functional diagram

The present paper is focused on MTG FCI visible detection chain. After describing the detection chain itself and the main specification driving the design, the test setup will be overviewed, followed by electrical and preliminary radiometric on-ground test results performed on a visible detection chain breadboard model (BBM) will be presented to validate the design choices and interfaces aspects.

I. DETECTOR CHAIN DESCRIPTION AND MAIN SPECIFICATIONS:

It is composed of a Visible Detecteur Assembly (VisDA) manufactured by e2v and a 12 bits resolution specific visible VCU operating in full-differential mode. The visible detector chain contains 5 channels in the wavelength range 414nm to 924nm. A very large rhombus pixel shape with dimensions of up to 100µm has been chosen to optimize both the MTF and SNR performances. The pixel shape allows to independently reach North/South and East/West MTF performance and minimise aliasing effect. The radiometric performance

maximization is achieved thanks to the rhombus geometrical extension and the noise minimization using CDS (correlated Double Sampling) at pixel level. For operability reason, the sensitive areas include 4 pixel columns (one nominal and 3 redundant) with one active pixel per line, which can be selected by Serial Programming Interface on request. The whole visible detection chain has been designed for high linearity (target $\pm 1.5\%$) and stability (target $\pm 0.05\%$) during the entire mission. A particular attention has been paid to optimize the spectral template and reduce the etalon effect. A black coating film has been deposited to lower reflectivity on the die surface and improve the straylight performance. Finally, a low lag performance has been demonstrated despite the large size of the pixel [3] to be compatible with a specification of 0.1% temporal remanence at instrument level.

The VCU contains a FEE (Front End Electronic) integrating the functions of video amplification, clock drivers and low noise biases (see Fig. 2). It is interfaced with the redounded VAE (Video acquisition Electronic describe in Fig. 2), which includes the ADC conversion, the generation of the clocks, SPI signal, supply voltages, and the management of the redounded thermal sensor. The VCU ensure the interface with the ICU (Instrument Control Unit).

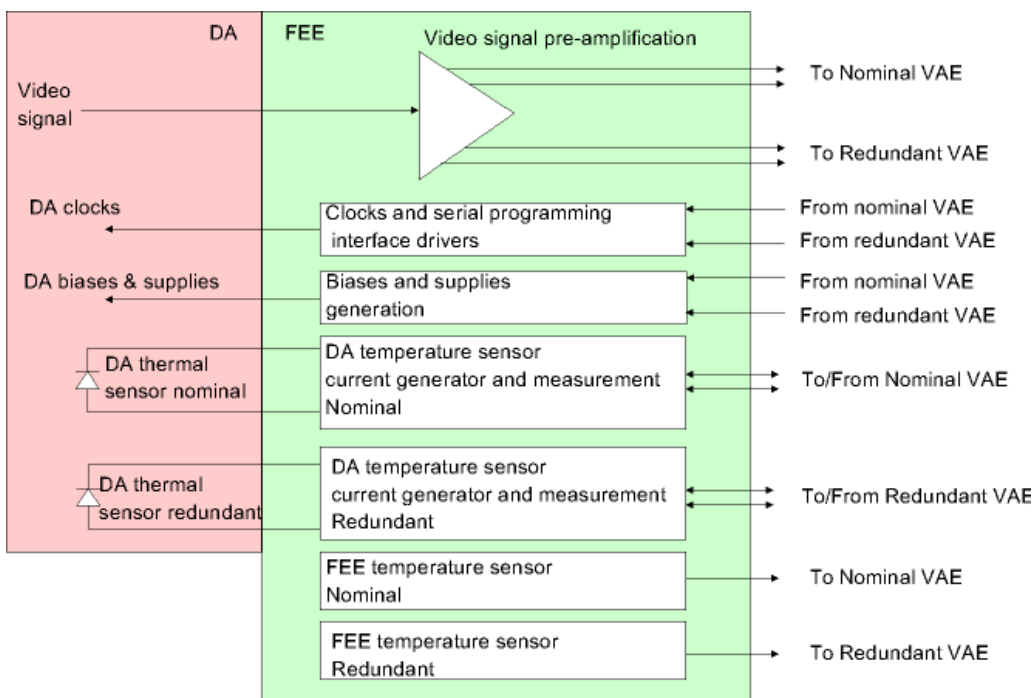


Fig. 2. FEE functional diagram

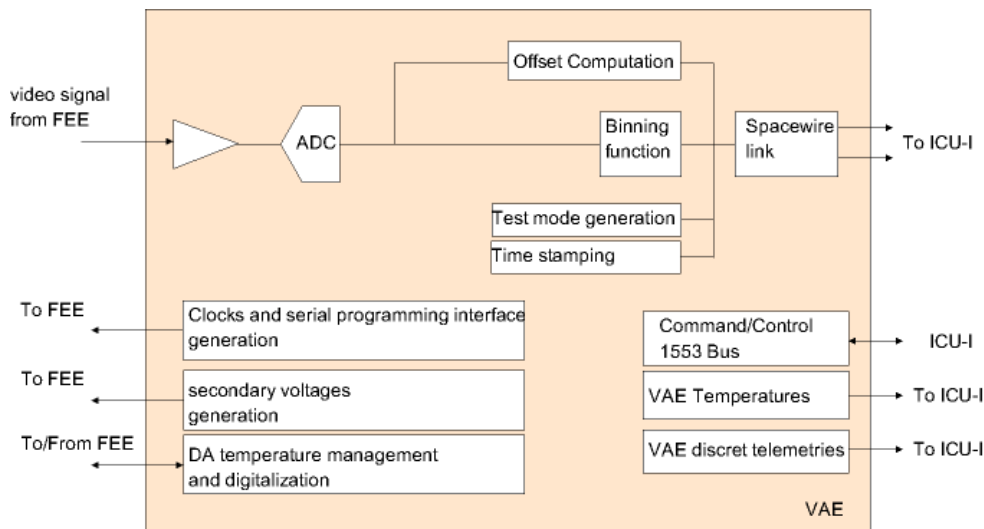


Fig. 3. VAE functional diagram

II. TEST BENCHES DESCRIPTION

The Test Bench is a set of optical, mechanical and electrical elements that allow to carrying out radiometric characterization of VisDA detector. This configuration aims also to test the functionalities of the detection chain composed of the VisDA and the VCUs.

Light is generated by a halogen lamp with well-defined spectral characteristics. A set of filters and diaphragm can tune the spectrum and light intensity to be injected in the integrating sphere. The spatially uniform output optical signal feeds a light sensor to monitor the optical source radiance. The VisDA is enclosed in a box exhibiting a narrow aperture to avoid stray-light. The control of the equipment and boards, such as the control of the optical source and power meter, is carried out by a customized LABVIEW software, using different communication ports (USB, GPIB, RS232).

The following scheme describes the test bench functionalities: optical source subsystem with this control/command electronic (green), visible detection chain (red), detector thermal system (Blue), and Test bench control Command system (Black):

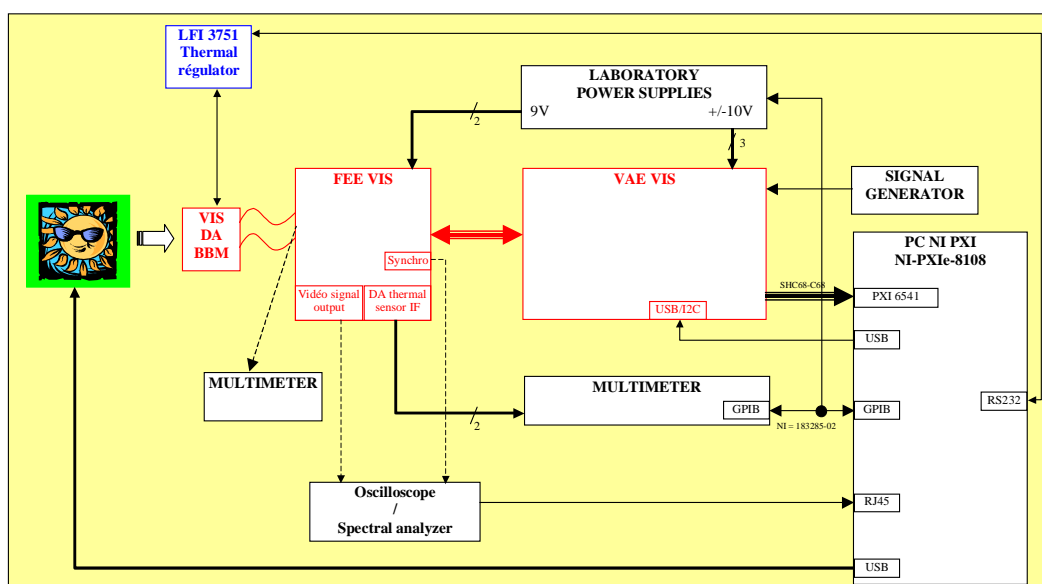


Fig. 4. Test bench functional scheme

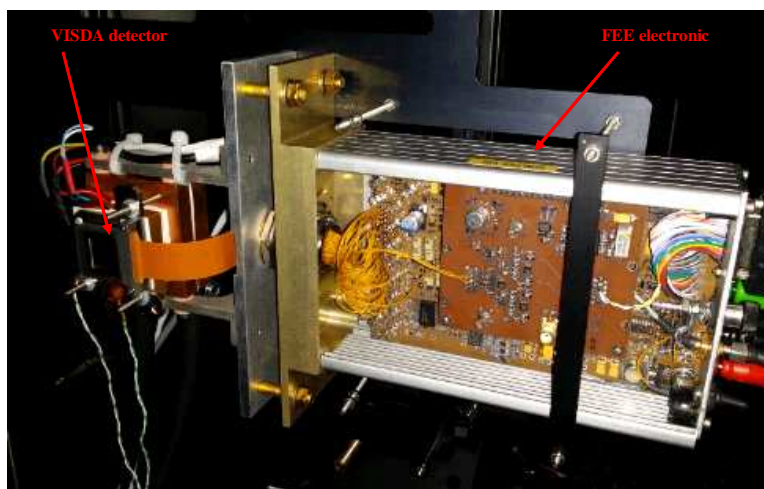


Fig. 5. Visible detection chain BBM photograph

The visible detection chain BBM is shown in Fig. 5. The BBM performance and interfaces are electrically representative, however not optically as no filter assembly has been manufactured in the VisDA. The radiometric measurements performed by this test bench are summarized in the following table:

Parameters	Description
V_{dark} (V)	Mean Darkness Voltage for one column
DSNU (%) pp (peak to peak)	Dark Signal dispersion for one column
CVF	Voltage Conversion Factor
Nreadout (lsb) rms	Readout Noise for one column
PRNU (%) pp	Responsivity dispersion for one column
NL (%)	Mean linearity for one column
Nldiff (%) pp	Standard Deviation of linearity for one column
Vsat (lsb)	Saturation signal for one column
ΔV_{sat} (lsb) pp	Saturation signal dispersion for one column

III. PRELIMINARY RESULTS

The aim of the DA FCI BBM activities is to test and validate detection interface and to measure radiometric performance (mainly noise and linearity) in order to:

- Consolidate and validate all the VisDA, FEE and VAE functional and electrical interface requirements.
- Verify the detection chain main radiometric performance (especially noise and linearity).
- Consolidate the design before the CDR of the detection chain parts.

The test plan is described in the following figure:

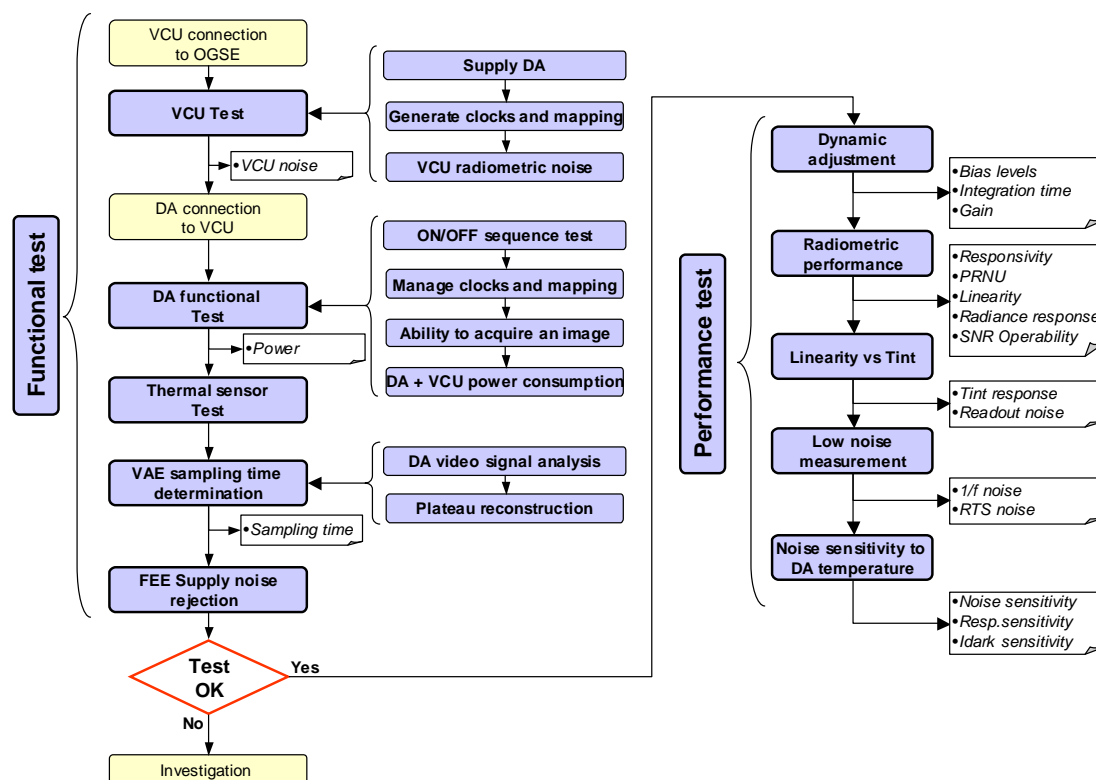


Fig. 5. Visible detection chain test plan

The current measurements have verified successfully the visible detection functional requirements. The radiometric measurements are in progress. The preliminary radiometric results are about:

- Dark noise:

The noise in darkness of the complete chain noise (Electronic Noise + Detector Noise) have been measured around 250-290 μ V rms for most of the channels, except for the channel centered at 914 nm (VisDA 0.9) which is higher (around 410 μ V rms) due to an additional electrical amplifier at pixel level. It has been also measured

that the dark current was negligible inside the detector. The values are determined by the standard deviation of 1000 acquisitions in darkness in the case of acquisition with an integration time equal to 228μs. The results are summarized in the following figure and table:

	VisDA 04	VisDA 05	VisDA 06	VisDA 08	VisDA 09
Output electrical gain (μV/LSB)	439,4	439,4	439,4	439,4	439,4
Measured electrical noise (LSB)	0,41	0,41	0,41	0,41	0,41
Measured electrical noise (μV rms)	180,9	180,4	179,9	180,0	179,9
Measured dark total noise (μV rms)	279,7	270,6	249,2	286,4	412,8

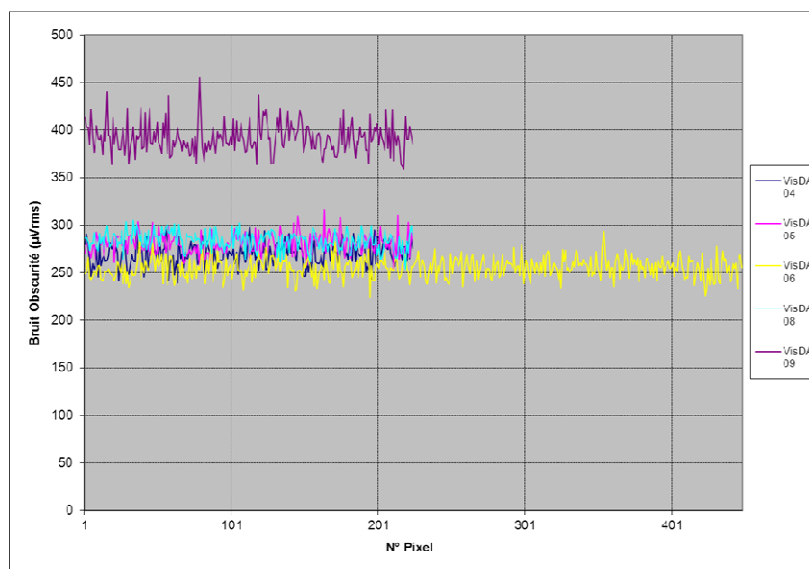


Fig. 6. Dark noise measurements

- Dark signal non uniformity:

The dark signal non-uniformity (DSNU) as usually defined cannot be measured due to a too low dark current and integration time limitation of the current TAS configuration of the electronic corresponding to a flight model. The following figure presents the video output signal spatial non uniformity for all pixels of each channel. The peak to peak dispersion ($= V_{c,j} - \bar{V}_c$ with c channel number and j pixel number) is around $\pm 2mV$ which is negligible with regards to the video output signal dynamic (e.g. represent less than 0.25% of the dynamic range) which confirm that the dark is negligible.

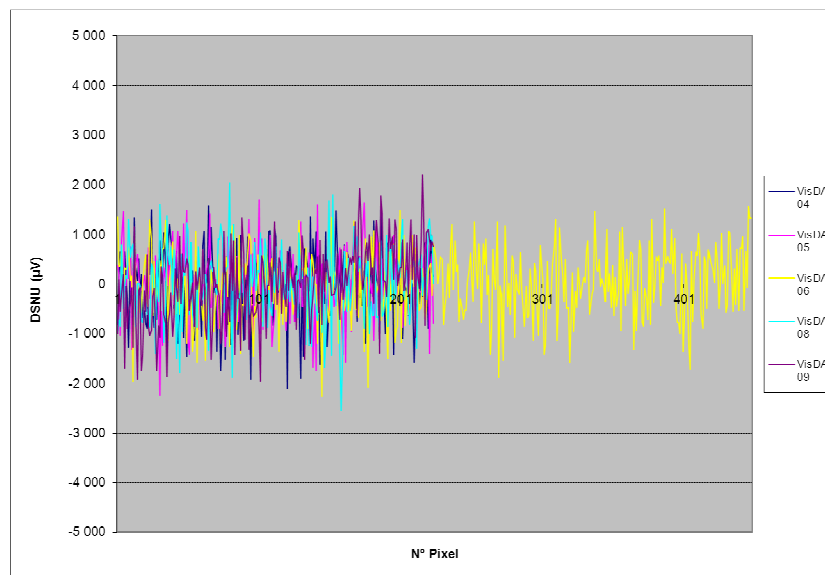


Fig. 7. Variation of signal in darkness ($= V_{c,j} - \bar{V}_c$) for the 5 visible channels (c).

- Responsivity dispersion:

The Photo-Response Non Uniformity (PRNU) is reported in this paragraph as the responsivity variation of all working pixels over the mean responsivity, divided by the mean responsivity of all working pixels. The measurements have been performed at half dynamic. The results summarized in the following figure and table demonstrate a PRNU lower than 3% for all channels.

	VisDA 04	VisDA 05	VisDA 06	VisDA 08	VisDA 09
$Min\left[\frac{Resp_{c,j} - \overline{Resp_c}}{\overline{Resp_c}}\right]$ in %	-0,8%	-0,7%	-0,5%	-0,8%	-1,6%
$Max\left[\frac{Resp_{c,j} - \overline{Resp_c}}{\overline{Resp_c}}\right]$ in %	1,7%	0,8%	0,6%	0,7%	1,2%
Max - Min in %	2,5%	1,5%	1,0%	1,5%	2,8%

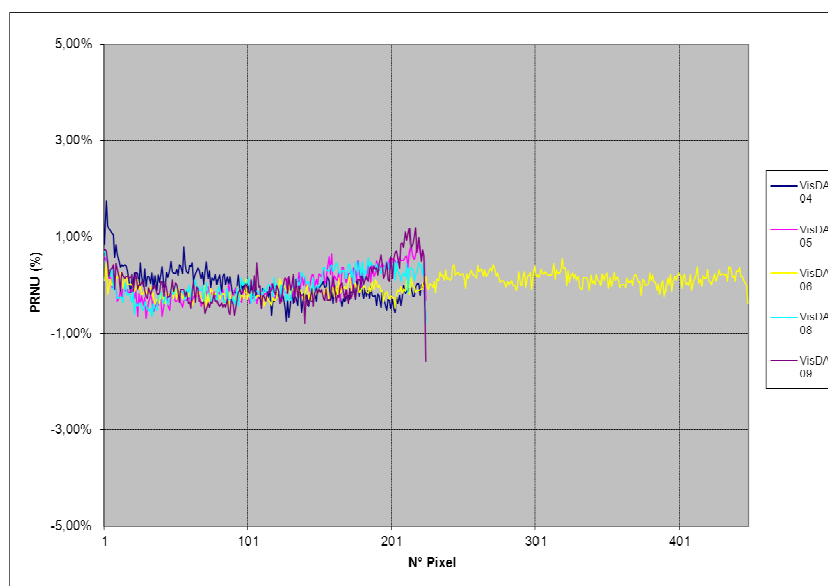


Fig. 8. Photoresponse variation measurements

- 1/f noise

The 1/f noise has been estimated by computation of the Noise Power Spectral Density (NPSD) of a continuous acquisition of 11s (30000 frames) in darkness condition. This time correspond to maximum time duration between to offset correction at beginning of each of a scanline of the earth at the equator. Thanks to the CDS (Correlated Double Sampling), no 1/f noise has been identified with frequency higher than 0.09 Hz as shown in the following figure for one representative channel.

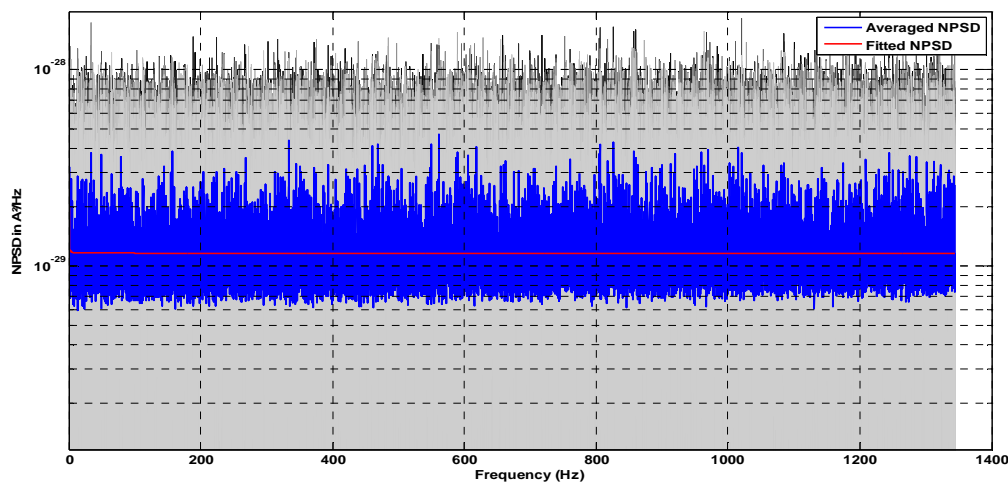


Fig. 9. NPSD measurements of all Vis0.9 pixels with in blue the average NPSD in blue and the fit in red

- RTS noise

The Random Telegraph Signals (RTS) noise is characterized by sudden jumps in in the video output signal in spatial and temporal domain. The measurement consists of performing 120 acquisitions in darkness condition of 1000 frames every 10s and compute for each acquisition the average and noise level for each pixel. This acquisition sequence corresponds to two times the full scan of the earth allowing to detect pixel in sudden jump. A pixel is declared in RTS when: the average difference between two consecutive acquisitions is higher than 10 times the median level of all pixels, and the noise difference between two consecutive acquisitions is higher than 1.3 times the median level of all pixels. VisDA is not been affected by RTS noise. The following figure presents the result for a representative channel.

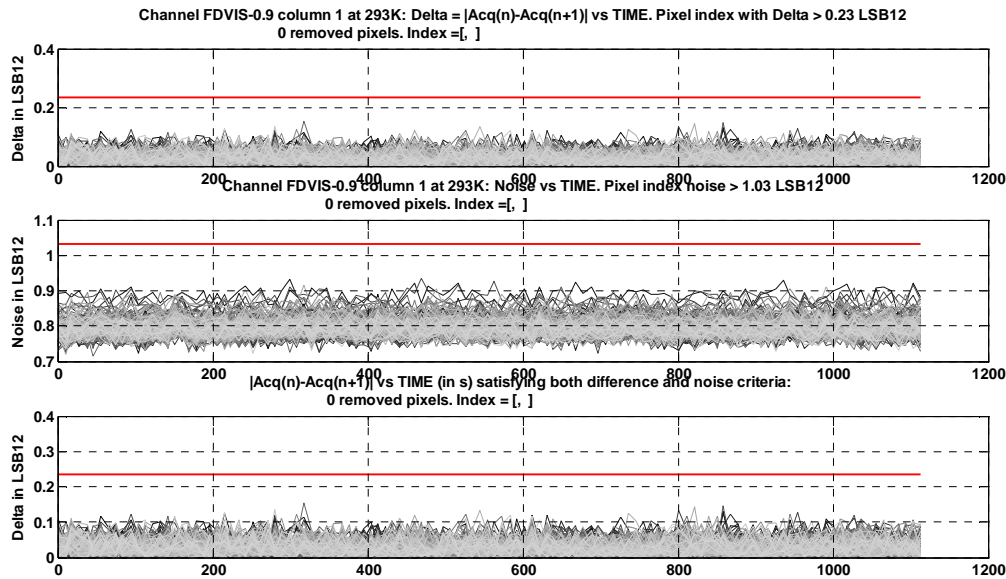


Fig. 9. RTS measurements

- Linearity measurement:

The linearity measurement are reported in the following figure. The curves have been computed based on a first order polynomial least mean square method. The error bars represent the pixel to pixel dispersion. The values are around 1% more than the expected target of $\pm 1.5\%$, except at low flux (e.g. for video output level lower than 0.2V) where the non-linearity is more important in the VisDA, limited by the CMOS sensor. A compensation method should be envisaged to overcome this behavior.

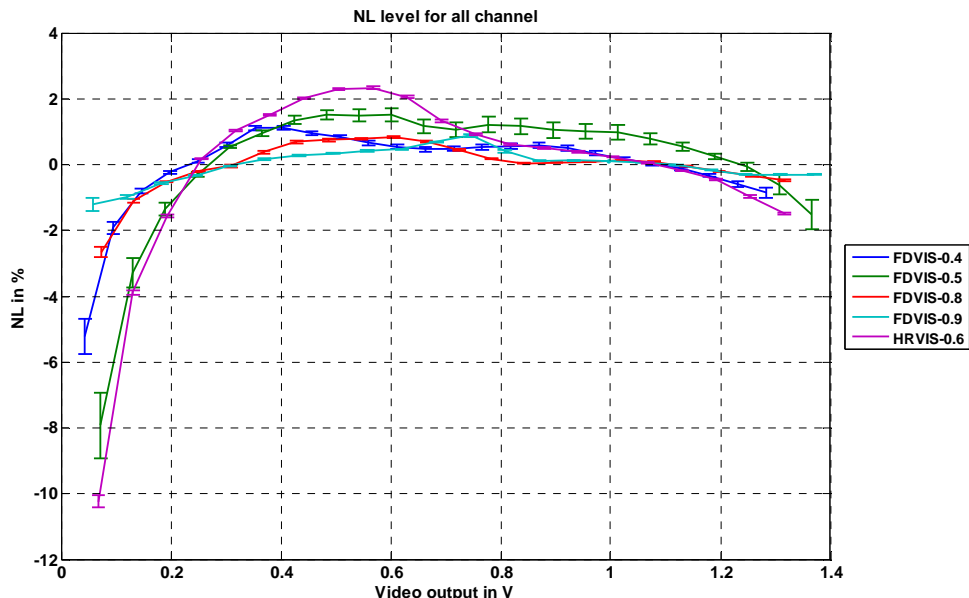


Fig. 10. Linearity measurements

CONCLUSION

The visible detection chain breadboard results are very encouraging and have fulfilled most of the objective. Functional and electrical interface requirements have been consolidated and validated between the VisDA and the VCU. The preliminary characterized detection chain radiometric performance (e.g. noise, DSNU, PRNU, linearity, $1/f$ and RTS noise) are globally within the expectations. Measurements are in progress to determine the conversion voltage factor (CVF) and the signal to noise ratio (SNR).

This first measurement campaign has then demonstrated the first working visible detection chain based on CMOS image sensor technology for MTG program. The inputs of these results will be used to secure the final visible detection chain design, considering that a filter assembly will be integrated inside the VisDA.

TAS would like to thank e2v and TAS Spain for their technical support and for having manufactured the VisDA and VCU respectively.

REFERENCES

- [1] Donny M. Aminou, Hendrik Stark, Wolfgang Schumann, Gary Fowler, Stefano Gigli, Antonio Rodríguez, "Meteosat Third Generation: progress on space segment system feasibility studies: payload aspects," Proceedings of SPIE, 'Sensors, Systems, and Next-Generation Satellites XI,' Vol. 7106, Cardiff, Wales, UK, DOI:10.1117/12.800244, Sept. 15, 2008
- [2] J. Ouaknine, T. Viard, B. Napierala, U. Foerster, S. Fray, P. Hallibert, Y. Durand, S. Imperiali, P. Pelouas, J. Rodolfo, F. Riguet, J-L. Carel, "The FCI on-board MTG: Optical Design and Performances" ICSO conference, October 7-10, 2014.
- [3] J. Pratlong, A Pike, W Hubbard, P Jerram, F. Mayer, B. Diasparra, B. Gili, R. Guiguet, S. Demiguel, J.L. Canaud, and M. Wilson, "MTG FCI Visible Detector design and development", Workshop CMOS Image Sensors for High Performance Applications, CNES Toulouse France, 26th and 27th November 2013.